Available online at www.sciencedirect.com
SCIENCE DIRECT®
Thermochimica Acta 426 (2005) 61–72
thermochimica acta
www.elsevier.com/locate/tca

Synthesis and thermal decomposition of freeze-dried copper–iron formates

F. Kenfack[1], H. Langbein*

Department of Chemistry, Institute of Inorganic Chemistry, Dresden University of Technology, Helmholtzstr. 10, D-01069 Dresden, Germany

Received 7 June 2004; received in revised form 23 July 2004; accepted 25 July 2004
Available online 9 September 2004

Abstract

The thermal decomposition of freeze-dried formate precursors for copper–iron oxides was investigated by means of DTA, TG, mass spectroscopy and X-ray powder diffractometry. The freeze-dried copper formate is crystalline. Its decomposition at about 200 °C releases formic acid (HCOOH) and carbon dioxide (CO_2) as main primary gaseous decomposition products beside metallic copper as a solid product. However, the decomposition of the amorphous freeze-dried iron formate starts with a dehydration process which ends up at about 200 °C. Further decomposition in several superimposed steps, between 220 °C and 330 °C, results in the delivery of: (a) HCOOH and CO_2 (with reduction of Fe(III) to Fe(II)), (b) HCOOH and CO or H_2CO and CO_2 (without reduction). Meanwhile, several secondary decomposition products are characterized by mass spectroscopy. Regarding the complex copper–iron formate, its decomposition does not reflect only some aspects of the single formates, but also an interaction between the components which lows down the decomposition temperature. Because of the intermediate formation of metallic copper, properties of the reactive homogeneous precursor are lost and the formation of the single-phase copper iron oxides requires an annealing temperature close to that of a mixed oxide technique.

Keywords: Copper–iron oxides; Freeze-drying; Formate precursor; Thermal analysis; Mass spectroscopy

1. Introduction

During the last few decades, the synthesis of the single-phase "$CuFe_2O_4$" has been a subject of intense investigations. Both ceramic and chemical methods have been used. Mexmain [1], Brabers and Klerk [2] and Tang et al. [3] have prepared $CuFe_2O_4$ using a solid state reaction between copper oxide (CuO) and iron oxide (Fe_2O_3). Brezeanu et al. [4–8] have studied the thermal decomposition of the precursor $[Fe_2Cu(C_2O_4)_2(OH)_4(H_2O)_2]$ obtained by hydrolytic decomposition of the $FeC_2O_4{\cdot}2H_2O$–$Cu(CH_3COO)_2{\cdot}H_2O$ mixtures or by a precipitation reaction. These authors found that the specific architecture of the trinuclear coordination compound allows the direct synthesis of $CuFe_2O_4$ at a relatively low temperature. On the same footing, the thermal decomposition of a mixed copper iron oxalate, prepared by coprecipitation, has been investigated by Coetzee et al. [9]. For the preparation of thin films of $CuFe_2O_4$, Despax et al. [10] have used the coprecipitated mixed oxalate "$Cu_{1/3}Fe_{2/3}C_2O_4{\cdot}2H_2O$". The increasing number of contributions mentioned above simply shows that preparing a pure copper ferrite is not easy. In fact at low temperature, special oxidizing/reductive atmospheres are required [1,11] and at high temperature ($T \geq 800$ °C), "$CuFe_2O_4$" contains CuO as second phase [1,2,10]. In our previous work [12], on the thermal decomposition of the freeze-dried precursor ammonium copper iron oxalate (Cu:Fe = 1:2), we were able to show that an individual decomposition of metal oxalates inside the precursor prevents the synthesis of a single spinel-phase "$CuFe_2O_4$" at low temperature ($T \leq 400$ °C). Kol-

* Corresponding author. Tel.: +49 351 463 34366; fax: +49 351 463 37287.
E-mail addresses: flaur@chemie.tu-dresden.de (F. Kenfack), Hubert.Langbein@chemie.tu-dresden.de (H. Langbein).
[1] Tel.: +49 351 463 34960.

0040-6031/$ – see front matter © 2004 Elsevier B.V. All rights reserved.
doi:10.1016/j.tca.2004.07.008

eva et al. [13] have used copper–manganese formate solid solutions as precursors for copper manganese oxides. Polla and co-workers [14,15] have synthesized Cu–Ca and Cu–Sr oxides by thermal decomposition of appropriate mixed formates. Note that investigations carried out in [13–15] preferentially aimed at the formation of oxidic phases and, the decomposition processes were discussed only on the basis of summarizing schematic equations. More recently, it has been shown [16] that the preparation of manganese ferrite with the freeze-dried precursor manganese iron formate "$MnFe_2O(CHOO)_6(H_2O)_3$" occurs at low temperature (T = 600 °C). In this work, we attempt instead to use copper–iron(III) formate as a precursor for the direct synthesis of pure copper ferrite. Specifically, we aim to enlighten relationships between the thermal decomposition of freeze-dried copper–iron formates and the formation of solid copper iron oxide phases. Thus, the thermal decomposition of Cu–Fe formate is compared to that of individual metal formates and the effect of the calcination temperature on the phase formation is studied. Besides, it is worth to emphasize that the thermal analysis coupled with mass spectrometry is a promising method to investigate the decomposition behaviour [16].

2. Experimental

For the freeze-drying process, complex formate solutions were firstly prepared. Fe(III) formate solution (A) was prepared as described by Langbein et al. [16]. Iron metal was dissolved with an appropriate amount of formic acid in an inert atmosphere. The resulting Fe(II) formate solution was then oxidized in a 10^{-2} M formic acid solution with a twofold excess of H_2O_2. Upon stirring the former solution, a deep brown Fe(III) formate solution was formed. Copper formate solution (B) was obtained by dissolving the basic copper carbonate ($CuCO_3 \times Cu(OH)_2 \cdot H_2O$) in an appropriate amount of formic acid. The metal ion concentrations of these solutions were determined titrimetrically to be 0.18 M and 0.09 M, respectively. A solution containing Cu^{2+} and Fe^{3+} in a molar ratio of Cu:Fe = 1:2 (C) was prepared using the previous solutions. Solutions (A, B and C) were quickly frozen in liquid nitrogen and dried from −40 °C to 25 °C in a vacuum chamber of a freeze-drying apparatus Alpha 2-4 (Christ). The quantitative analysis of the slight powders obtained was realised by complexometric titration and elemental analyses. Following these results, their composition can be described approximately using these formulas:

$$\text{iron formate} : [Fe_3O(HCOO)_6]^{+}HCOO^{-} \cdot 3.8H_2O;$$

$$\text{copper formate} : Cu(HCOO)_2 \cdot 0.1H_2O;$$

$$\text{copper–iron formate} : \text{“}CuFe_2O_{2/3}(HCOO)_{6.67} \cdot 2.5H_2O\text{”}$$

$$[2/3\,[Fe_3O(HCOO)_6]{+}HCOO^{-},\ 1\,Cu(HCOO)_2,\ 2.5\,H_2O].$$

In dependence on the conditions during the freeze-drying process and, after handling in air with different humidity, the water content of the samples can be somewhat different.

From the X-ray diffraction analysis (Fig. 1), the freeze-dried iron(III) formate is amorphous, the copper formate is crystalline while the copper–iron formate is partially amorphous, with traces of crystalline copper formate. Analysing of the IR spectra of freeze dried amorphous Fe(III) formate, it turns out that at least partially complex trinuclear μ–oxo formate species are present. Such complexes are well known for crystalline iron carboxylates [17].

X-ray diffraction analysis was performed with a Siemens D5000 X-ray diffractometer using Cu Kα radiation. The ther-

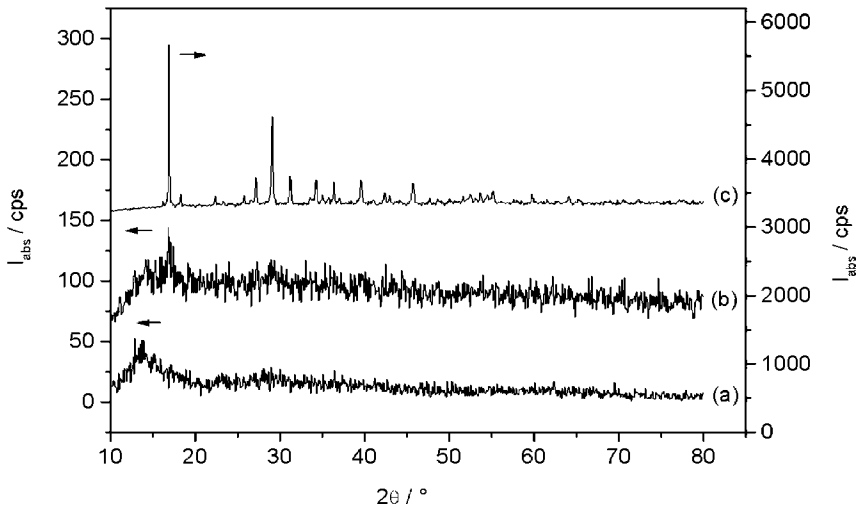

Fig. 1. XRD patterns of the freeze-dried precursors: (a) Fe formate "$[Fe_3O(HCOO)_6]^{+}HCOO^{-} \cdot 3.8H_2O$"; (b) Cu–Fe formate "$CuFe_2O_{2/3}(HCOO)_{6.67} \cdot 2.5H_2O$"; and (c) Cu formate "$Cu(HCOO)_2 \cdot 0.1H_2O$".

mal decomposition was investigated by means of Netzsch thermal analyser STA 409, coupled with a capillary mass spectrometer QMG 420 (Balzers).

3. Results and discussion

3.1. Iron(III) formate precursor

The thermal decomposition of the freeze-dried precursor iron(III) formate in an argon gas stream is illustrated in Fig. 2. The decomposition starts with an endothermic process corresponding to about 13% mass loss in the TG curve. This process is superimposed by the beginning of an exothermic decomposition occurring between 200 °C and 290 °C and characterized by two substeps on the DTG. The last process is an endothermic one with a maximum at about 325 °C. Above 330 °C, a small gain of mass by the products is observed. The total mass loss including the small gain of mass is about 57%.

To elucidate the mechanism of decomposition, the gaseous decomposition products were analysed by mass spectrometry. The results of this measurement are recorded in Table 1 and plotted in Fig. 3a and b.

The mass spectroscopic analysis of gaseous products permits to conclude that at least five parallel and/or consecutive reactions occur during the four decomposition steps identified on the DTA and DTG curves (Table 1). One sees that the decomposition starts with the elimination of H_2O (process (1)). The calculated mass loss (12.1%) corresponding to the loss of 3.8 mol of water for each mole of precursor is found to be lower than the experimental value (about 13%). This suggests that the formation of HCOOH and CO_2 (process (2a)) is superimposed to the process (1).

$$[Fe_3O(HCOO)_6]^+HCOO^- \cdot 3.8H_2O \rightarrow [Fe_3O(HCOO)_6]^+HCOO^- + 3.8H_2O \quad (1)$$

$$[Fe(III)_3O(HCOO)_6]^+HCOO^- \rightarrow [Fe(III)_2Fe(II)O(HCOO)_6] + 0.5HCOOH + 0.5CO_2 \quad (2a)$$

$$[Fe(III)_2Fe(II)O(HCOO)_6] \rightarrow [Fe(II)_3O(HCOO)_4] + HCOOH + CO_2 \quad (2b)$$

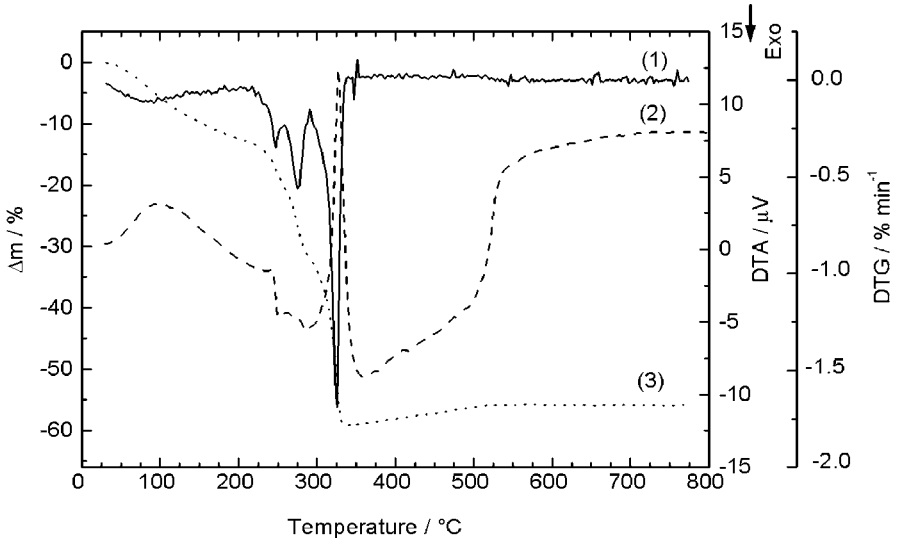

Fig. 2. Thermal analysis of the freeze-dried Fe formate "$[Fe_3O(HCOO)_6]^+HCOO^- \cdot 3.8H_2O$": (1) DTG curve; (2) DTA curve; and (3) TG curve. Atmosphere: argon; heating rate: 5 K/min.

Table 1
Main primary gaseous decomposition products of the freeze-dried precursor $[Fe_3O(HCOO)_6]^+HCOO^- \cdot 3.8H_2O$

Process/equation	Temperature range (°C), roughly	Main primary gaseous decomposition products	Δm (calc.) (%)	
			Δm/step	Δm/total
1	30–220	$3.8H_2O$	−12.1	−12.1
2a	200–260	$0.5HCOOH; 0.5CO_2$	−7.9	−20.0
2b	240–290	$HCOOH; CO_2$	−15.9	−35.9
3	280–330	$2HCOOH; 2CO$	−26.1	−62.0
4	280–330	$2H_2CO; 2CO_2$	−26.1	−62.0
	330–520	(oxidation)	+4.2	−57.8

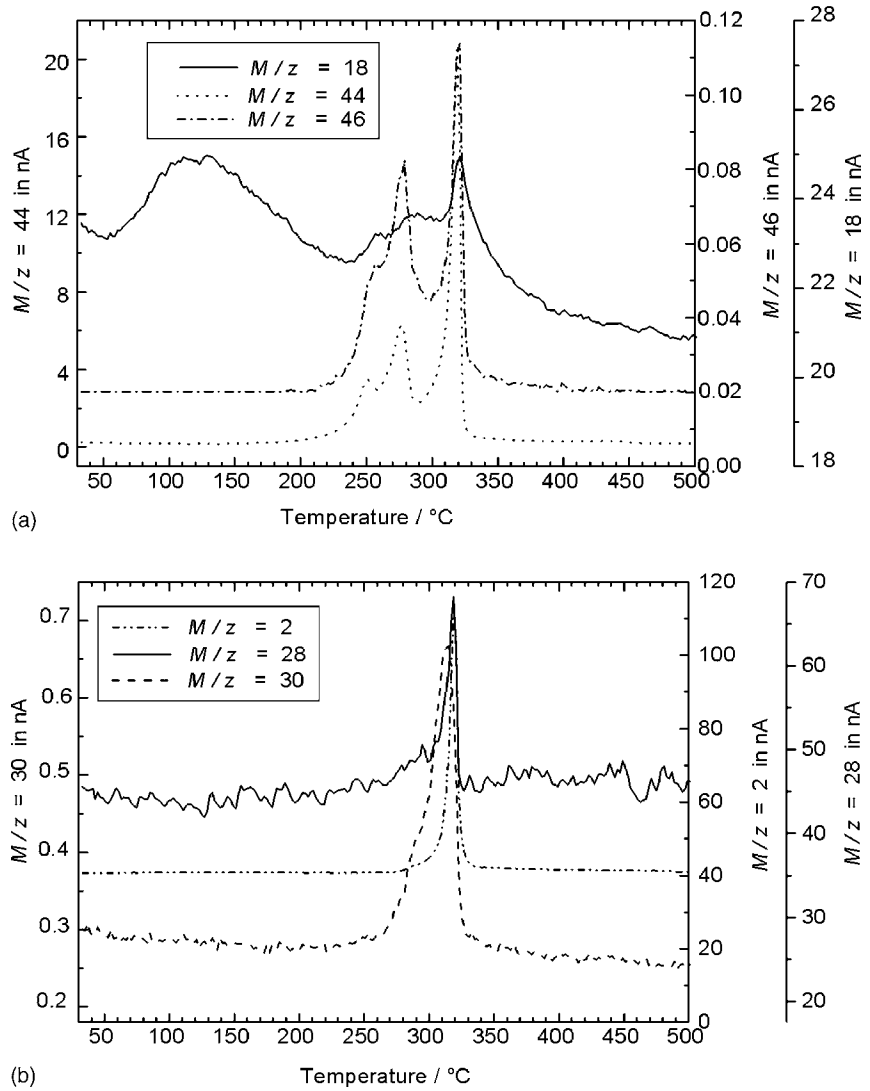

Fig. 3. (a) Mass spectrometry characterization of the gaseous decomposition products occurring during the decomposition of the freeze-dried Fe formate "$[Fe_3O(HCOO)_6]^+HCOO^-\cdot 3.8H_2O$". Atmosphere: argon; heating rate: 5 K/min. m/z = 18 (H_2O); m/z = 44 (CO_2); and m/z = 46 (HCOOH). (b) Mass spectrometry characterization of the gaseous decomposition products occurring during the decomposition of the freeze-dried Fe formate "$[Fe_3O(HCOO)_6]^+HCOO^-\cdot 3.8H_2O$". Atmosphere: argon; heating rate: 5 K/min. m/z = 2 (H_2); m/z = 28 (CO); and m/z = 30 (HCOH).

HCOOH and CO_2 result from an electron transfer from the formate anion to Fe(III) and from the reaction of two HCOO-moieties via an H-transfer from one to the other. The decomposition proceeds with the process (2b). In this process, which is analogous to (2a), a further reductive elimination with the delivery of HCOOH and CO_2 takes place.

As the temperature increases, the competitive processes (3) and (4) become more and more important. Contrary to processes (2a) and (2b), they occur without alteration of the oxidation number of iron.

$$[Fe(II)_3O(HCOO)_4] \rightarrow 3FeO + 2HCOOH + 2CO \quad (3)$$

$$[Fe(II)_3O(HCOO)_4] \rightarrow 3FeO + 2H_2CO + 2CO_2 \quad (4)$$

The formation of HCOOH and CO or H_2CO and CO_2 can be explained by the breaking of Fe–O and O–C bonds in the trinuclear molecular units according to the schematic Eqs. (5) and (6) and by H-transfer reactions between the resulting HCOO and HCO radicals.

$$(R)Fe–O(CO)H \rightarrow (R)Fe–O^{\bullet} + HC^{\bullet}O \quad (5)$$

$$(R)Fe–O(CO)H \rightarrow (R)Fe^{\bullet} + HCOO^{\bullet} \quad (6)$$

From the reaction between the simultaneously formed $(R)Fe–O^{\bullet}$ and $(R)Fe^{\bullet}$ species, Fe–O–Fe links arise. This should result in the formation of wüstite, "FeO", as a final solid product. At about 300 °C, wüstite is a metastable iron oxide in relation to a Fe/Fe_3O_4 mixture. But, its formation by decomposition of a Fe(II) compound at relatively low temperature is not unusual. Analogous decomposition processes were also identified during the decomposition in argon of the freeze-dried precursor Mn–Fe formate [16].

The small gain of mass between 330 °C and 520 °C is caused by the reoxidation of Fe(II), formed during the decomposition, by traces of oxygen in the argon gas stream (see below). After finishing the thermal analysis at about 800 °C, hematite (α-Fe_2O_3) is formed as a solid product.

During all the decomposition processes, a delivery of H_2O is observed. Beside this, H_2 is detected above 300 °C. These facts can be explained by decomposition processes in accordance with Eqs. (7)–(9).

$$HCOOH \rightarrow H_2O + CO \quad (7)$$

$$HCOOH \rightarrow H_2 + CO_2 \quad (8)$$

$$H_2CO \rightarrow H_2 + CO \quad (9)$$

The decomposition processes (8) and (9) are important only above 300 °C, whereas the reaction (7) had already taken place above 200 °C. Because of the simultaneous presence of CO, CO_2, H_2O and H_2 in the reaction system, the existence of further equilibriums like (10) and (11) are expected.

$$CO + H_2O \leftrightharpoons CO_2 + H_2 \quad (10)$$

$$2CO \leftrightharpoons CO_2 + C \quad (11)$$

Reaction (10) is discussed by Maciejewski et al. [18] as H_2 forming process during the decomposition of $Co(C_2O_4)\cdot 2H_2O$. The Boudouard reaction (11) could explain the presence of traces of carbon in the solid decomposition product up to about 700 °C.

According to Dollimore and Tonge [19], there are two main routes for the decomposition of anhydrous metal formates $M(OOCH)_2$ to metal oxides MO at temperatures $T >$ 400 °C: formation of (a) 2CO and H_2O and (b) CO, CO_2 and H_2 in addition to MO. Peshev and Pecheva [20] have investigated the thermal dissociation of a crystalline complex trinuclear iron(III) formate in inert atmosphere by gas chromatographic analysis between 340 °C and 350 °C. They have characterized H_2O, CO, CO_2 and H_2 as gaseous decomposition products. The results of [19] and [20] are fully in agreement with our results. However, a careful investigation as a function of the temperature with mass spectroscopic detection of products allows some further conclusions concerning the single processes and their primary gaseous products.

To confirm the thermal analysis results, various thermal treatments were performed in the range of 30–800 °C. The resulting solid products were characterized using the X-ray diffraction method. In order to proceed, defined amounts (100–150 mg) of Fe(III) formate were decomposed under argon. After reaching the desired temperature, the samples were quenched rapidly to room temperature under the same atmosphere. From the examination of the XRD profiles obtained at selected temperatures (260 °C, 300 °C, and 340 °C), one can note that the thermal reactions defined from the DTA, TG and MS results, are approved (Fig. 4). After annealing up to 260 °C (step (2a)), a less crystalline iron formate is formed from the amorphous freeze-dried precursor (Fig. 4, curve a). After further reduction of iron during the annealing process up to 300 °C (step 2b), another crystalline formate is formed. The most intensive peak at about 22 = 14.5° coincides with the two most intensive nearly neighbouring peaks of iron(II) formate (PDF 20-0514) (Fig. 4, curve b). Obviously, the crystallization processes are related to the exothermic peaks at about 260 °C and 290 °C in the DTA curve (Fig. 2). Additionally, it is observed that at 300 °C, the crystallization of iron oxides begins. At the end of the decomposition process (340 °C), metastable wüstite "FeO" (minor phase) and magnetite (Fe_3O_4) are formed (Fig. 4, curve c). Note that small differences in the reaction conditions can affect the wüstite/magnetite ratio. There are two possible reasons for the appearance of magnetite beside wüstite: (a) before the

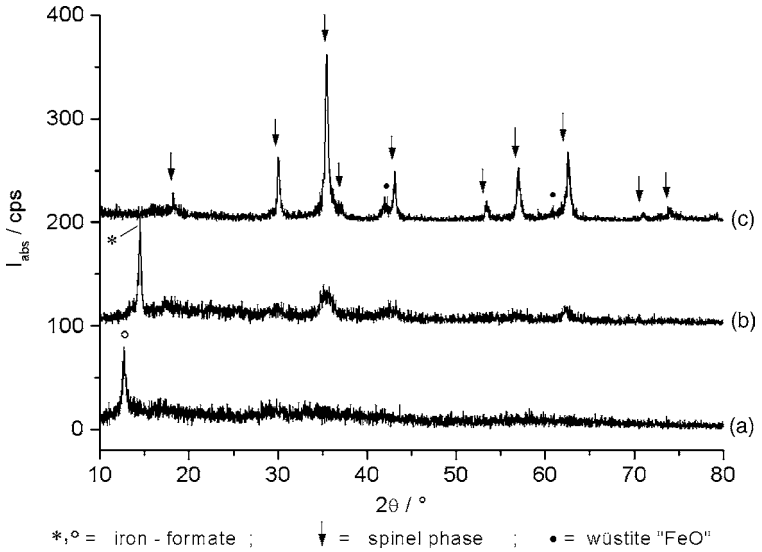

Fig. 4. XRD patterns of the decomposition products of the freeze-dried Fe formate "$[Fe_3O(HCOO)_6]^+HCOO^-\cdot 3.8H_2O$" quenched after annealing at: (a) 260 °C; (b) 300 °C; and (c) 340 °C. Atmosphere: argon; heating rate: 5 K/min.

interruption of the decomposition process at 340 °C, a partial reoxidation of wüstite has already passed off or (b) more probable, in competition and superimposed to processes (2b) between 240 °C and 290 °C and processes (3) and (4) between 280 °C and 330 °C, a further decomposition without further reduction of Fe(III) takes place, according to parallel reactions (12a), (13a) and (12b), (13b), respectively.

$$[Fe(III)_2Fe(II)O(HCOO)_6] \rightarrow [Fe(III)_2Fe(II)O_2(HCOO)_4] + HCOOH + CO \quad (12a)$$

$$[Fe(III)_2Fe(II)O(HCOO)_6] \rightarrow [Fe(III)_2Fe(II)O_2(HCOO)_4] + H_2CO + CO_2 \quad (13a)$$

$$[Fe(III)_2Fe(II)O_2(HCOO)_4] \rightarrow Fe_3O_4 + 2HCOOH + 2CO \quad (12b)$$

$$[Fe(III)_2Fe(II)O_2(HCOO)_4] \rightarrow Fe_3O_4 + 2H_2CO + 2CO_2 \quad (13b)$$

The thermal decomposition proceses summarized in Table 1 and discussed above are in agreement with the TG/DTA/MS results. Because of the large number of different superimposed primary and secondary processes and the large number of different products and their mass spectroscopic fragments, exact conclusions concerning the portion of single processes are not possible. The actual yield in each reaction product is very sensitive to the experimental conditions.

The decomposition of the iron(III) formate in air atmosphere occurs in only two observable steps (Fig. 5). The decomposition also starts with the endothermic release of coordinated water (process1, between 30 °C and 220 °C). All the further processes are superimposed by the oxidation of the primary decomposition products. This results in an altogether exothermic process in a narrow temperature range (maximum of the DTA curve at 273 °C). From the X-ray diffractogram pattern obtained after decomposition up to 290 °C, the resulting solid phase is maghemite, γ-Fe_2O_3 (Fig. 6, curve a). The primary formation of magnetite and its reaction to γ-Fe_2O_3 is also expected. In this way, wüstite and magnetite formed during the decomposition in argon can also be transformed to maghemite. During all these transformations, the cubic close-packed arrangement of the oxide anions is preserved. Above 400 °C, the metastable maghemite is transformed to the thermodynamically stable hematite, α-Fe_2O_3 (Fig. 6, curve b).

3.2. Copper formate precursor

Depending on the preparation conditions, dehydrated copper formate can be obtained in three different crystalline forms [21]. Our freeze-drying process results in a nearly dehydrated crystalline product with a monoclinic structure. The X-ray powder diffractogram is shown in Fig. 7, curve a. It is in agreement with PDF 32-331. The same form is obtained by dehydration of copper(II) formate tetrahydrate [22].

The TG, DTG and DTA were employed to investigate the decomposition of the freeze-dried copper formate, $Cu(HCOO)_2 \cdot 0.1H_2O$, in argon and in air atmosphere (Fig. 8). The TGA curves show about 1.2% mass loss upon heating up to ∼180 °C. This mass loss which is accompanied by two less intensive endothermic peaks in the DTA curve (Fig. 8, curve 1) is due to the dehydration of copper formate. Between 190 °C and 220 °C, the total decomposition of the formate takes place. For the decomposition in argon, the total mass loss at 215 °C correlates with the formation of copper metal (Δm_{calc} = −59.1%). This agrees with the X-ray powder diffractogram of the sample annealed up to 220 °C. Copper metal is formed as the main crystalline substance (Fig. 7, curve b). The gain of mass above 220 °C is caused by the reoxidation of copper metal by traces of oxygen in the argon atmosphere (Δm_{calc} = + 10.3%). From the experimental gain of mass observed between 230 °C and 750 °C,

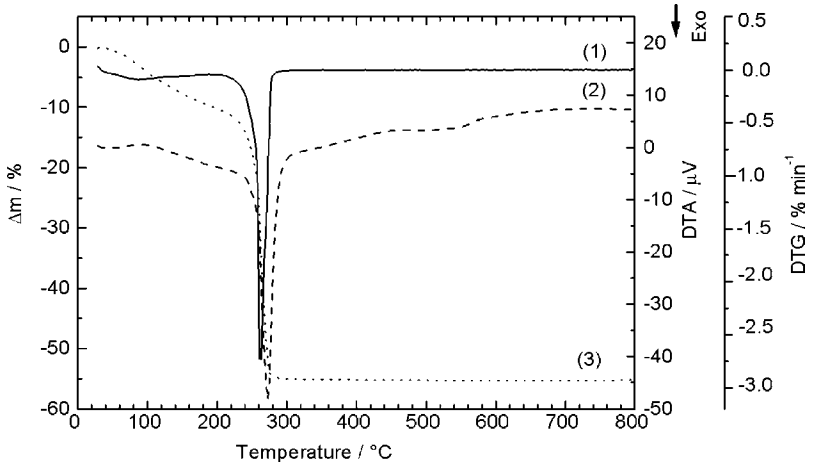

Fig. 5. Thermal analysis of the freeze-dried Fe formate "$[Fe_3O(HCOO)_6]^+HCOO^- \cdot 3.8H_2O$": (1) DTG curve; (2) DTA curve; and (3) TG curve. Atmosphere: air; heating rate: 5 K/min.

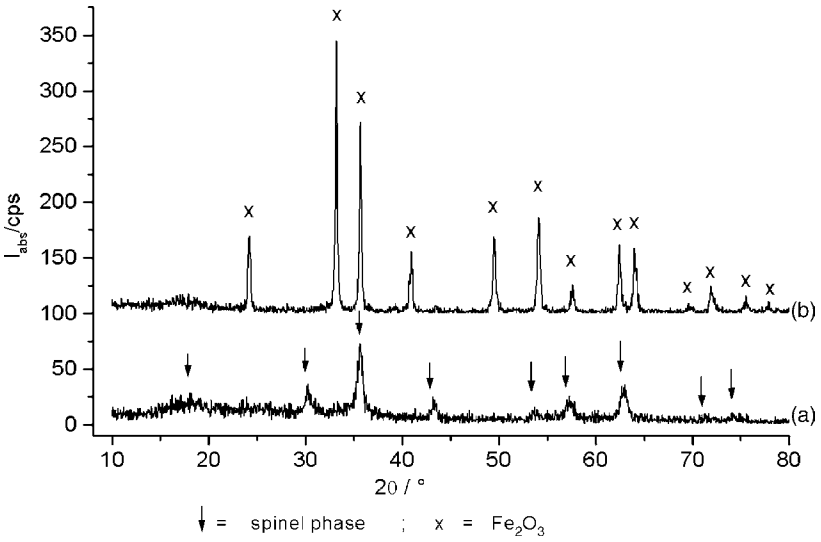

Fig. 6. XRD patterns of the decomposition products of the freeze-dried Fe formate "$[Fe_3O(HCOO)_6]^+HCOO^-\cdot 3.8H_2O$" quenched after annealing at: (a) 290 °C; and (b) 600 °C. Atmosphere: air; heating rate: 5 K/min.

it turns out that, up to 750 °C, the total oxidation of copper is not yet occurred. The resulting product is constituted of Cu_2O and a remaining amount of Cu (Fig. 7, curve c). The broad exothermic peak in the DTA curve above 250 °C should be the result of the slow oxidation of Cu and crystallization of Cu_2O. Because of numerous different processes between 200 °C and 250 °C (decomposition and crystallization processes) the DTA peaks in this region do not allow any further detailed discussion. In air atmosphere, indicated by the maximum mass loss of only 57%, the reoxidation begins before the full decomposition and ends at about 400 °C. The altogether mass loss is in agreement with the calculated value of $\Delta m_{calc} = -48.8\%$ (Fig. 8, curve 3).

The main gaseous decomposition products in argon are CO_2, H_2O, CO, H_2 and HCOOH (Fig. 9). As in the reductive decomposition of iron formate (2a) and (2b), the primary process in the decomposition of the dehydrated copper formate should be the formation of HCOOH and CO_2 (14). The decomposition of HCOOH results in the formation of H_2O and CO (7) or H_2 and CO_2 (8). Unlike the decomposition of the freeze-dried iron formate, H_2 is formed at about 200 °C. The reaction (7) is probably enhanced kinetically. Including a catalytic activity of a fine grained copper metal, formed during the decomposition of copper formate, the reaction (8) can already be important at a much lower temperature. The detection of minor amounts of H_2CO should be the result of the reaction $HCOOH + CO \leftrightharpoons H_2CO + CO_2$ or the result of a side reaction without reduction, analogously to reaction (4).

$$Cu(HCOO)_2 \rightarrow Cu + HCOOH + CO_2 \quad (14)$$

A stepwise decomposition of anhydrous copper formate, reported in [23], with a first step already at 110 °C (forma-

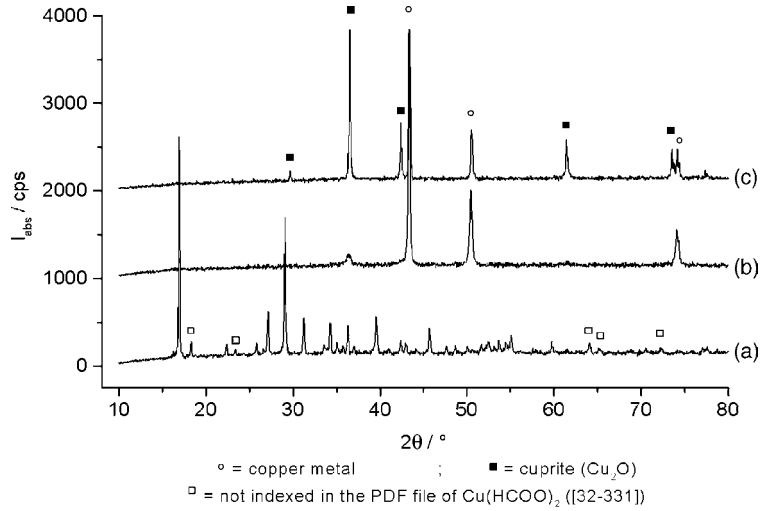

Fig. 7. XRD patterns of: (a) the freeze-dried Cu formate "$Cu(HCOO)_2\cdot 0.1H_2O$" and of the decomposition products quenched after annealing at: (b) 220 °C; and (c) 750 °C. Atmosphere: argon; heating rate:5 K/min.

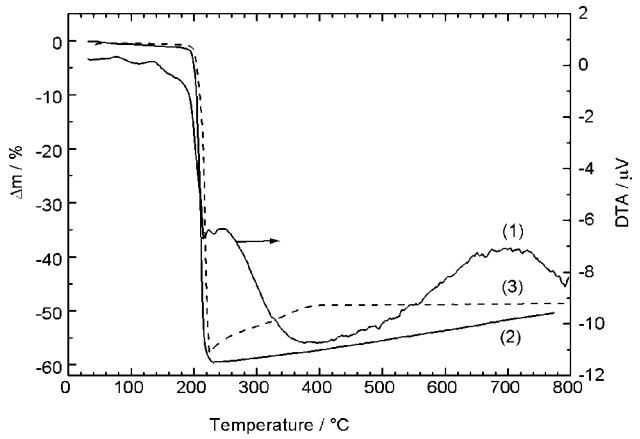

Fig. 8. Thermal analysis of the freeze-dried Cu formate "$Cu(HCOO)_2 \cdot 0.1H_2O$": (1) DTA curve in argon; (2) TG curve in argon; and (3) TG curve in air. Heating rate: 5 K/min.

tion of a Cu(I) compound), could not be observed. In [23] a orthorhombic copper formate (PDF 32-332), obtained by a special preparation was decomposed. This is a reference to a different decomposition behaviour for different crystalline forms of copper formate.

3.3. Copper–iron formate precursor

The thermal decomposition of the freeze-dried precursor copper–iron formate occurs in three more or less superimposed steps in the range 30–290 °C (Fig. 10). The decomposition starts with an endothermic delivery of water (30–220 °C) (process (1)). One notes that the initial and the final temperatures of further decomposition are located between these of the single formates. This reflects interactions between the components of the freeze-dried product. According to the results of the decomposition of individual Fe(III) formate/Cu formate (3.1 and 3.2), the second step (210–250 °C) overall exothermic, is related to the superposition of three processes: the reduction of Cu^{2+} to Cu yielding to the release of HCOOH (m/z = 46) and CO_2 (m/z = 44) (Eq. (14)), the reduction of Fe(III) to Fe(II) also leading to the release of HCOOH and CO_2 (Eq. (2a)) and the further decomposition of the iron component without reduction, forming HCOOH and CO (according Eq. (12a)) or H_2CO (m/z = 30) and CO_2 (Eq. (13a)). The superimposed third step (250–290 °C), overall endothermic, characterizes the total decomposition of Fe(II/III) formate nearly without a further reduction of Fe(III). In this step, the competition processes described by the Eqs. (12b) and (13b) occur simultaneously (Table 2, Fig. 11a and b). Analogously to the decomposition of single formates, the intensities of the mass spectroscopic peaks of the primary decomposition products HCOOH and H_2CO are much lower than the intensities of the peaks of secondary products. But, unlike the decomposition of the iron formate precursor, the development of H_2 begins at about 220 °C. That means in the case of the complex formate, the consecutive reactions (8) and (9) are important at this temperature. This should be caused by the catalytic activity of the metallic copper.

The altogether mass loss of about 60% at 290 °C correlates very well with the expectation for ((2/3)Fe_3O_4 + Cu). Above 290 °C, the product is progressively oxidized by the traces of oxygen in argon atmosphere. Because of the numerous strongly superimposed processes, summarized in Table 2, no reaction scheme is given. The decomposition behaviour reflects the characteristics of the decomposition of the single compounds. Because of the "dilution" of the copper component, their decomposition begins at a somewhat higher temperature, and, the catalytic influence of the arising copper metal results in a favoured decomposition of the iron formate component.

According to the X-ray powder diffraction analysis, one sees that the results obtained from the TG/MS are clearly approved (Fig. 12). After annealing up to 240 °C, crystalline

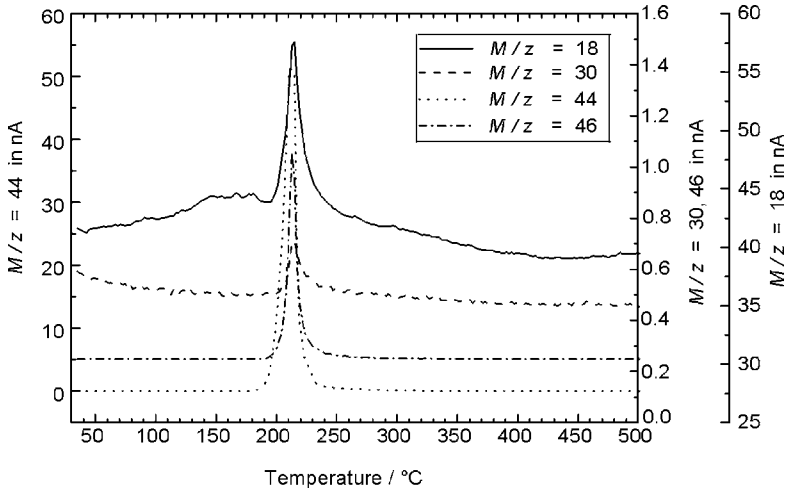

Fig. 9. Mass spectrometry characterization of the gaseous decomposition products occurring during the decomposition of the freeze-dried Cu formate "$Cu(HCOO)_2 \cdot 0.1H_2O$". Atmosphere: argon; heating rate: 5 K/min. m/z = 18 (H_2O); m/z = 30 (HCOH); m/z = 44 (CO_2); and m/z = 46 (HCOOH).

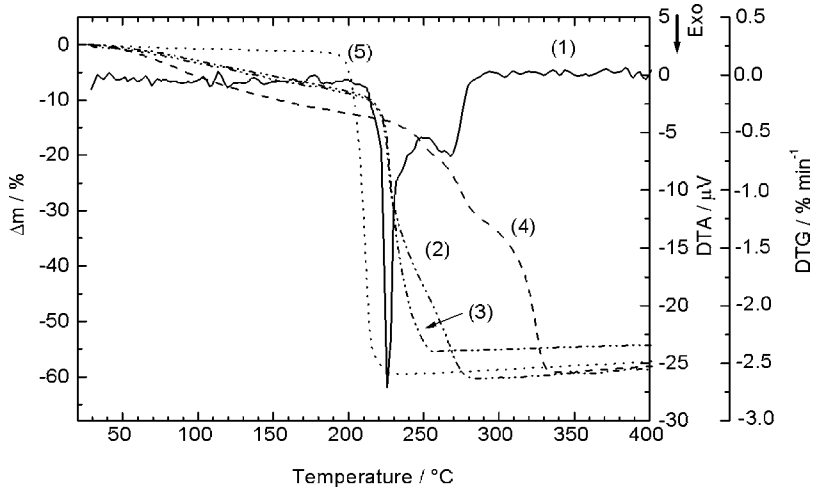

Fig. 10. Thermal analysis of the freeze-dried Cu–Fe formate "$CuFe_2O_{2/3}(HCOO)_{6.67}\cdot 2.5H_2O$": (1) DTG curve in argon; (2) TG curve in argon; (3) TG curve in air; and (4) TG curve in argon of the freeze-dried Fe formate "$[Fe_3O(HCOO)_6]^+HCOO^-\cdot 3.8H_2O$"; (5) TG curve in argon of the freeze-dried Cu(II) formate "$Cu(HCOO)_2\cdot 0.1H_2O$". Heating rate: 5 K/min.

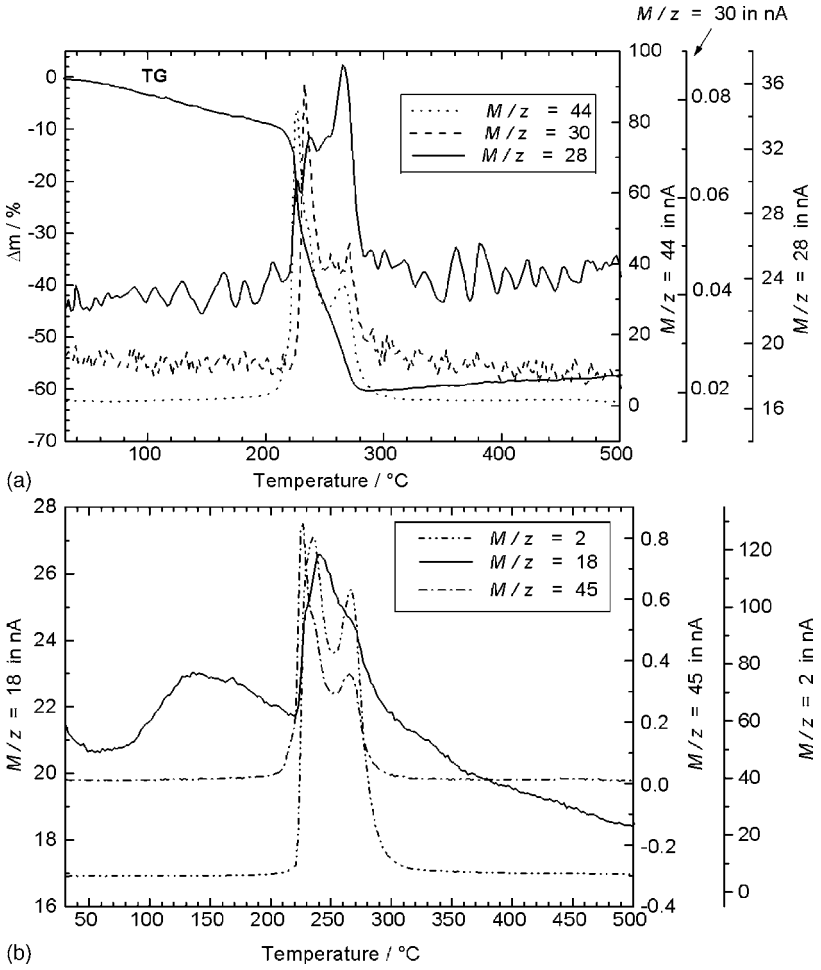

Fig. 11. (a) Thermal analysis of the freeze-dried Cu–Fe formate "$CuFe_2O_{2/3}(HCOO)_{6.67}\cdot 2.5H_2O$" and mass spectrometry characterization of the gaseous decomposition products. Atmosphere: Argon; heating rate: 5 K/min. m/z = 28 (CO); m/z = 30 (HCOH); and m/z = 44 (CO_2). (b) Mass spectrometry characterization of the gaseous decomposition products occurring during the decomposition of the freeze-dried Cu–Fe formate "$CuFe_2O_{2/3}(HCOO)_{6.67}\cdot 2.5H_2O$". Atmosphere: argon; heating rate: 5 K/min. m/z = 2 (H_2); m/z = 18 (H_2O); and m/z = 45 (HCOO fragment).

Table 2
Main primary gaseous decomposition products of the freeze-dried precursor [(2/3)([$Fe_3O(HCOO)_6$]$^+$ $HCOO^-$), $Cu(HCOO)_2$, $2.5H_2O$]

Process/equation	Temperature range (°C), roughly	Main primary gaseous decomposition products	Δ*m* (calc.) (%)	
			Δ*m*/step	Δ*m*/total
1	30–220	$2.5H_2O$	−8.5	−8.5
12	210–250	HCOOH; CO_2	−17.0	−25.5
2a	210–250	(2/3)(0.5HCOOH; $0.5CO_2$)	−5.7	−31.2
10a	210–250	(2/3)(HCOOH; CO)	−9.3	−40.5
11a	210–250	(2/3)(H_2CO; CO_2)	−9.3	−40.5
10b	250–290	(2/3)(2HCOOH; 2CO)	−18.6	−59.1
11b	250–290	(2/3)($2H_2CO$; $2CO_2$)	−18.6	−59.1
	290–600	Oxidation	+2.5	−56.6

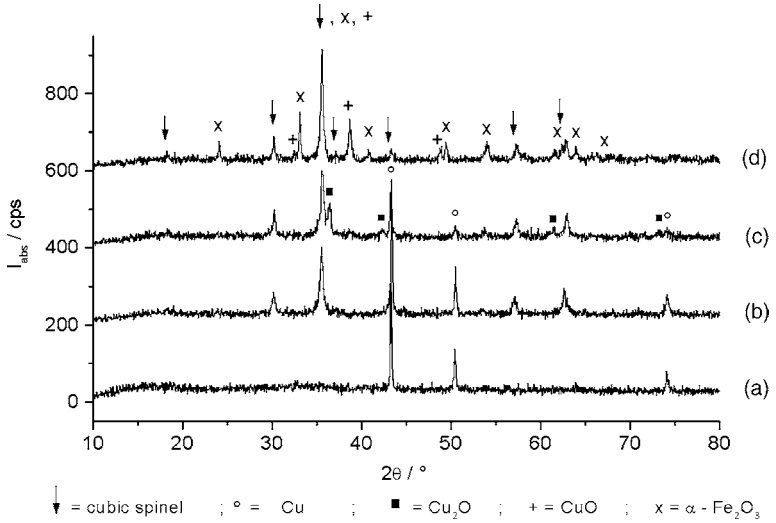

Fig. 12. XRD patterns of the decomposition products of the freeze-dried Cu–Fe formate "$CuFe_2O_{2/3}(HCOO)_{6.67}\cdot 2.5H_2O$" quenched after annealing at: (a) 240 °C; (b) 320 °C; (c) 400 °C; and slowly cooled after annealing at: (d) 400 °C during 24 h. Atmosphere: argon; heating rate: 5 K/min.

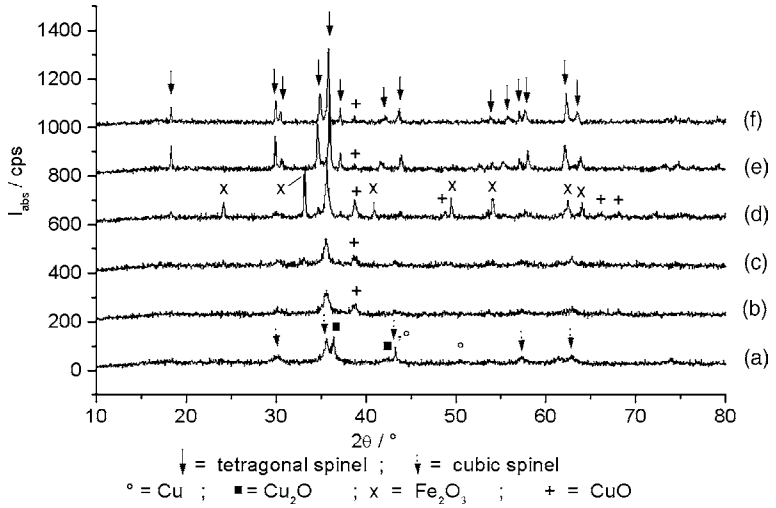

Fig. 13. XRD patterns of the decomposition products of the freeze-dried Cu–Fe formate "$CuFe_2O_{2/3}(HCOO)_{6.67}\cdot 2.5H_2O$" quenched after annealing at: (a) 260 °C; (b) 400 °C; and slowly cooled after annealing during 24 h at: (c) 400 °C; (d) 600 °C; (e) 800 °C; and (f) 1000 °C. Atmosphere: air; heating rate: 5 K/min.

metallic copper is present beside the amorphous iron component (Fig. 12, curve a). Further annealing up to 320 °C leads to the additional formation of the spinel-phase Fe_3O_4 (Fig. 12, curve b). Contrarily to the decomposition of the single iron formate, no wüstite phase is detectable. The continuation of the annealing process results in the slow oxidation of copper ($Cu \rightarrow Cu_2O \rightarrow CuO$) and magnetite ($Fe_3O_4 \rightarrow \gamma\text{-}Fe_2O_3$) by traces of oxygen in the argon atmosphere. After 24 h of thermal treatment at 400 °C, the metastable spinel compound $\gamma\text{-}Fe_2O_3$ is transformed partially to $\alpha\text{-}Fe_2O_3$. The formation of some copper poor-spinel phase ($Cu_{1-x}Fe_2O_{4-\delta}$) beside the aforementioned phases is expected (Fig. 12, curves c and d).

The thermal decomposition of the freeze dried Cu–Fe formate in air atmosphere (Fig. 10, curve 3) also starts with the endothermic delivery of water. In the temperature range 200–260 °C, the decomposition of the anhydrous formate takes place. The simultaneous oxidation of the gaseous products results in the formation of CO_2 and H_2O and, altogether, the decomposition process is strongly exothermic. The small gain of mass above 260 °C indicates that the reoxidation of copper metal and iron(II) begins during the decomposition process. At 260 °C, the solid product contains a less crystalline cubic spinel compound (copper poor spinel-phase $Cu_{1-x}Fe_2O_{4-\delta}$ and/or $\gamma\text{-}Fe_2O_3$), copper metal (small amount) and cuprite (Cu_2O) (Fig. 13, curve a). After annealing up to 400 °C, Cu and Cu_2O are fully oxidized to CuO (Fig. 13, curve b). During 24 h of annealing at 400 °C, the separation of $\alpha\text{-}Fe_2O_3$ begins (Fig. 13, curve c). This separation is continued up to 600 °C. Upon annealing at 600 °C, the solid state reaction between $\alpha\text{-}Fe_2O_3$ and CuO starts (Fig. 13, curve d). This reaction ends between 800 °C and 1000 °C and results, after a slow cooling process, to a tetragonal copper ferrite (Fig. 13, curves e and f). Due to the partial reduction of Cu(II) to Cu(I) in this temperature range, the product contains an iron rich spinel-phase $Cu_{1-x}Fe_{2+x}O_4$ and a small amount of CuO. This is in agreement with results of our investigations concerning the synthesis of copper ferrites by oxidation of metallic precursors described in [24].

4. Conclusions

The thermal decomposition of freeze-dried iron(III) formate, copper(II) formate and copper(II)–iron(III) formate includes an intermediate reduction of the metal ions. Regarding copper–iron(III) formate, the resulting product of decomposition in argon contains copper metal and an iron oxide with spinel structure $Fe^{3+}_{(8/3-2x)}\square_{1/3-x}Fe^{2+}_{3x}O_4$. The value of x depends on the scale of oxidation by traces of oxygen after decomposition ($x = 0$ for maghemite and $x = 1/3$ for magnetite). In air atmosphere, the reoxidation begins during the decomposition process. After decomposition up to 400 °C, the solid product contains a poor crystalline spinel beside CuO (Fig. 13, curve b). A raw calculation of the lattice constant of the spinel-phase gives $a_0 = 8.36$ Å. This value is situated between the lattice constants of $\gamma\text{-}Fe_2O_3$ ($a_0 = 8.34$ Å) and that of $CuFe_2O_4$ ($a_0 = 8.37$ Å). It follows that the poor crystalline spinel phase contains some copper. Analogously to the maghemite–hematite transformation, further heating leads to the separation of hematite (Fig. 13, curves c and d).

The freeze-dried copper iron formate can be characterized as a mixture of an amorphous iron formate component and a small amount of crystalline copper formate (Fig. 1). But the poor-crystallinity in comparison with the freeze-dried copper formate and its decomposition behavior reflect an interaction between the metal formate components in the very homogeneous freeze-dried precursor. Despite this fact, the direct synthesis of the copper ferrite with spinel structure at low temperature is prevented by the formation of copper metal during the decomposition process. Its reoxidation to CuO and the effective reaction with the iron oxide component requires a temperature higher than the γ–$\alpha\text{-}Fe_2O_3$ transformation temperature. It turns out that the synthesis of the copper ferrite should be performed only at higher temperature by a conventional solid state reaction. That means the advantage of the reactive homogeneous precursor can not yield in a low temperature synthesis of the complex oxide. This should also be a problem for other copper ferrite precursors which are likely to release reducing components during the decomposition.

The chance to form copper ferrite directly in a decomposition reaction is expected to be higher for heteronuclear $Cu–Fe_2$ complex compounds with an ideal homogeneity on the molecular level and (if possible) without reducing components. The realization of such precursors should be a goal of further investigations.

Acknowledgement

The authors would like to thank Mrs. H. Dallmann for performing measurements of thermal analysis and mass spectrometry.

References

[1] J. Mexmain, Ann. Chim. 4 (1969) 429.
[2] V.A.M. Brabers, J. Klerk, Thermochim. Acta 18 (1977) 287.
[3] X.X. Tang, A. Manthiram, J.B. Goodenough, J. Solid State Chem. 79 (1989) 250.
[4] M. Brezeanu, A. Antoniu, O. Carp, M. Andruh, R. Barjega, Rev. Roum. Chim. 40 (1995) 403.
[5] M. Brezeanu, A. Antoniu, O. Carp, c. Lepadatu, M. Andruh, F. Zalaru, C. Achim, A. Gheorghe, R. Barjega, Rev. Roum. Chim. 40 (1995) 213.
[6] G. Marinescu, L. Patron, O. Carp, L. Diamandescu, N. Stanica, A. Meghea, M. Brezeanu, J.-C. Grenier, J. Etourneau, J. Mater. Chem. 12 (2002) 3458.
[7] O. Carp, M. Brezeanu, E. Segal, J. Therm. Anal. 47 (1996) 1709.
[8] O. Carp, L. Patron, G. Marinescu, G. Pascu, P. Budrugeac, M. Brezeanu, J. Therm. Anal. Calorim. 72 (2003) 263.
[9] A. Coetzee, D.J. Eve, M.E. Brown, J. Therm. Anal. 39 (1993) 947.

[10] C. Despax, Ph. Tailhades, C. Baubet, C. Vilette, A. Rousset, Thin Solid Films 293 (1997) 22.
[11] E. Kester, B. Gillot, C. Villette, Ph. Tailhades, A. Rousset, Thermochim. Acta 297 (1997) 71.
[12] F. Kenfack, M. Al Daroukh, H. Langbein, Z. Anorg. Allg. Chem. 628 (2002) 2182.
[13] V. Koleva, D. Stoilova, D. Mehandjiev, J. Solid State Chem. 133 (1997) 416.
[14] A.G. Leyva, G. Polla, P.K. de Perazzo, H. Lanza, M.A.R. de Benyacar, J. Solid State Chem. 123 (1996) 291.
[15] G. Polla, A.G. Leyva, P.K. de Perazzo, H. Lanza, M.A.R. de Benyacar, J. Solid State Chem. 117 (1995) 145.
[16] H. Langbein, S. Christen, G. Bonsdorf, Thermochim. Acta 327 (1999) 173.
[17] M.K. Johnson, D.B. Powell, R.D. Cannon, Spectrochim. Acta 37A (1981) 995.
[18] M. Maciejewski, E. Ingier-Stocka, W.-D. Emmerich, A. Baiker, J. Therm. Anal. Calorim. 60 (2000) 735.
[19] D. Dollimore, K.H. Tonge, J. Inorg. Nucl. Chem. 29 (1967) 621.
[20] P. Peshev, M. Pecheva, Mater. Res. Bull. 13 (1978) 419.
[21] A.K. Galwey, D.M. Jamieson, M.E. Brown, J. Phys. Chem. 78 (1974) 2664.
[22] J.R. Günter, J. Solid State Chem. 35 (1980) 43.
[23] M.A. Mohamed, A.K. Galwey, S.A. Halawy, Thermochim. Acta 411 (2004) 13.
[24] F. Kenfack, H. Langbein, Cryst. Res. Technol. 39 (11) (2004), in press.